applied sciences

MDPI

Article

Performance Assessment and Optimization of the Ultra-High Speed Air Compressor in Hydrogen Fuel Cell Vehicles

Ting Shi [1] and Xueyuan Peng [1,2,*]

[1] School of Energy and Power Engineering, Xi'an Jiaotong University, Xi'an 710049, China; shiting0301@stu.xjtu.edu.cn
[2] State Key Laboratory of Multiphase Flow in Power Engineering, Xi'an Jiaotong University, Xi'an 710049, China
* Correspondence: xypeng@mail.xjtu.edu.cn

Abstract: Air compressors in hydrogen fuel cell vehicles play a crucial role in ensuring the stability of the cathode air system. However, they currently face challenges related to low efficiency and poor stability. To address these issues, the experimental setup for the pneumatic performance of air compressors is established. The effects of operational parameters on energy consumption, efficiency, and mass flow rate of the air compressor are revealed based on a Morris global sensitivity analysis. Considering a higher flow rate, larger efficiency, and lower energy consumption simultaneously, the optimal operating combination of the air compressor is determined based on grey relational multi-objective optimization. The optimal combination of operational parameters consisted of a speed of 80,000 rpm, a pressure ratio of 1.8, and an inlet temperature of 18.3 °C. Compared to the average values, the isentropic efficiency achieved a 48.23% increase, and the mass flow rate rose by 78.88% under the optimal operational combination. These findings hold significant value in guiding the efficient and stable operation of air compressors. The comprehensive methodology employed in this study is applicable further to investigate air compressors for hydrogen fuel cell vehicles.

Keywords: hydrogen fuel cell vehicles; centrifugal air compressor; Morris sensitivity analysis; multi-objectives optimization

Citation: Shi, T.; Peng, X. Performance Assessment and Optimization of the Ultra-High Speed Air Compressor in Hydrogen Fuel Cell Vehicles. *Appl. Sci.* **2024**, *14*, 1232. https://doi.org/10.3390/app14031232

Academic Editor: Nikolaos Koukouzas

Received: 10 January 2024
Revised: 30 January 2024
Accepted: 31 January 2024
Published: 1 February 2024

1. Introduction

In the contemporary world, there is a widespread exploration and integration of diverse forms of novel energy sources [1]. These alternatives are emerging as pivotal solutions to tackle climate change and meet the growing energy needs [2], offering expanded avenues for sustainable development [3]. Hydrogen fuel cell vehicles (HFCVs) are considered the greenest [4] and most sustainable technology [5], which employ proton exchange membrane fuel cells (PEMFCs) as the power generation device [6]. PEMFCs utilize hydrogen [7] and oxygen as reactants [8], resulting in only electrical energy and water as byproducts [9], so they are considered the most promising power generation technology in HFCVs [10]. The high-speed, oil-free centrifugal air compressor plays a crucial role as part of the cathode air system in HFCVs [11]. Nevertheless, the existing air compressors employed in hydrogen-powered vehicles encounter challenges related to increased energy consumption [12] and reduced mass flow rates [13].

Numerous researchers have conducted studies on achieving a high-efficiency operation of air compressors in hydrogen energy vehicles. Li et al. [14] proposed a tandem-bladed impeller method for passive flow control to enhance the stable operating range of the compressor, eliminating control costs or performance drawbacks. The results demonstrate that this method using tandem impellers can achieve a remarkable maximum operating range increase of 16.7%. Sun et al. [15] investigated the impact of humidity on compressor performance and its underlying mechanism theoretically and experimentally. An enhanced humidity correction model was developed utilizing a similarity criterion. The results indicated that elevated humidity levels lead to a decrease in the total pressure ratio and peak isentropic efficiency, causing a shift in the performance curve towards lower mass flow rates. Zhao et al. [16] used a semi-physical modeling approach to assess the operational characteristics of a centrifugal compressor, which is favored for automotive fuel cells due to its compact design. This model comprises numerous physical and empirical parameters that are notably challenging to ascertain. An interior-point optimization technique employing Newton iteration is employed to determine these parameters. Wan et al. [17] devised a design approach that enhances the empirical parameter method to meet the distinct demands of a fuel cell powertrain system. The authors delve into the interplay between the air compressor and the fuel cell system. The results indicated that the centrifugal compressor tends to function within an elongated and confined region characterized by a low flow coefficient and a high head coefficient. This operational tendency results in diminished efficiency and considerable losses in hydraulic and disc friction. Mirzaee et al. [18] explored surge or stall events within a centrifugal compressor and examined the contribution of tip clearance flow to the instability observed in this compressor. Based on a computational method, the study analyzes the flow dynamics within the centrifugal compressor. Liu et al. [19] constructed a hybrid semi-mechanical and semi-empirical air supply system model. This model was integrated into the fuel cell control system to dynamically regulate the centrifugal air compressor in line with the duty cycle of the engine. Furthermore, a compound feed-forward PID control approach was introduced for the air compressor. Fang et al. [20] conducted a detailed analysis of empirical models pertaining to the efficiency and mass flow rates of centrifugal compressors. The results demonstrated that existing models designed for vehicle engines and turbocharger centrifugal compressors do not sufficiently meet the requirements for centrifugal compressors, highlighting the necessity for accurate models tailored specifically to this application. Zhao et al. [21] introduced a control approach employing dynamic disturbance decoupling control for a centrifugal compression system. This system is responsible for delivering compressed air to fuel cells, facilitating the generation of electricity through hydrogen reactions. With its ultra-high speed, this compressor boasts remarkable performance, rendering it well-suited for transportation applications.

These investigations mentioned above studied the impact of the rotor, impeller, motor, and control on the performance enhancement of the air compressor. However, the sensitivity analysis of operational parameters on air compressor performance and multi-objective optimization are ignored. Moreover, the demands of the fuel cell stack on the air compressor vary in real time due to the complex and varied operating conditions. Therefore, it is quite necessary to study the impact of the operating parameters on the performance of the air compressor.

The Morris sensitivity analysis method has been effectively utilized in various applications and fields, such as engines [22], the environment [23], and construction [24]. Essentially, it involves exploring multidimensional spaces, offering strengths such as strong model adaptability, reliable outcomes, and rapid screening capabilities. Liu et al. [25] introduced a comprehensive sensitivity analysis that combined various global sensitivity analysis methods, the design of experiment algorithms and indicators, and sample size designs. This integrated system effectively screened sensitive parameters robustly and efficiently reduced the burden of parameter optimization. Xiong et al. [26] used a method for the inversion of mechanical parameters in arch dams, leveraging the sensitivity analysis of the Morris method and the Hooke-Jeeves algorithm. The results demonstrated that the Morris analysis can identify the critical factors. Based on the previous research, it was found that the Morris analysis has a significant effect on the multi-objective.

Addressing multi-factor and multi-objective optimization presents a complex nonlinear challenge. Conventional methods struggle to identify the optimal solution under multiple objectives. For example, the Taguchi method is only capable of solving single-objective problems [27]. However, the grey relational analysis method can effectively address engineering problems with multiple optimization objectives simultaneously. Wang et al. [28] proposed an approach that combines experimental design and grey relational analysis for addressing problems in multiple criteria decision-making. Zheng et al. [29] presented an uncomplicated yet dependable approach for evaluating and optimizing building envelopes during the conceptual phase. An enhanced grey relational projection method was introduced to determine the optimal building envelope solution. Furthermore, a combined weighting approach, amalgamating subjective and objective weighting methods, was employed to compute the weights of the factors and sub-factors. Kuo et al. [30] recommended employing grey relational analysis for multiple-attribute decision-making purposes for such problem-solving scenarios. This research demonstrates that grey relational analysis effectively addresses multi-objective optimization problems.

Therefore, in this paper, the experimental setup of the dynamic performance of an air compressor for application in hydrogen energy vehicles is built. The effects of operating parameters on the performance of the air compressor are obtained. Based on Morris global sensitivity, the influence grade of operating parameters on the performance of air compressors is identified to guide the control strategy effectively for efficient operation. Considering both the operating requirements and grey relational multi-objective optimization theory, the optimal operating combination of the air compressors with higher efficiency, larger mass flow, and low energy consumption is determined for the first time. Compared to the average value, the optimal combination is verified. The research results can be applied to guide the efficient and stable operation of compressors in HFCVs. The comprehensive methodology presented in this study is also applicable to other studies concerning compressors in HFCVs.

2. Methodology

2.1. Air Compressors in HFCVs

PEMFCs are the most promising green and sustainable power systems in HFCVs, as depicted in Figure 1. The anode hydrogen and cathode air undergo oxidation–reduction reactions within the fuel cell stack, generating electrical energy and water. In PEMFCs, the seamless integration of components, including the air compressor, fuel cell stack, hydrogen supply system, and control system, enables the efficient coordination and optimization of functions. This integration ensures that the air supply aligns with the dynamic demands of the fuel cell stack, optimizing oxygen delivery and electrochemical reactions. Additionally, synergies among components, such as integrating the air compressor with advanced control systems, allow real-time adjustments based on vehicle power requirements, enhancing the overall efficiency of the fuel cell system [6].

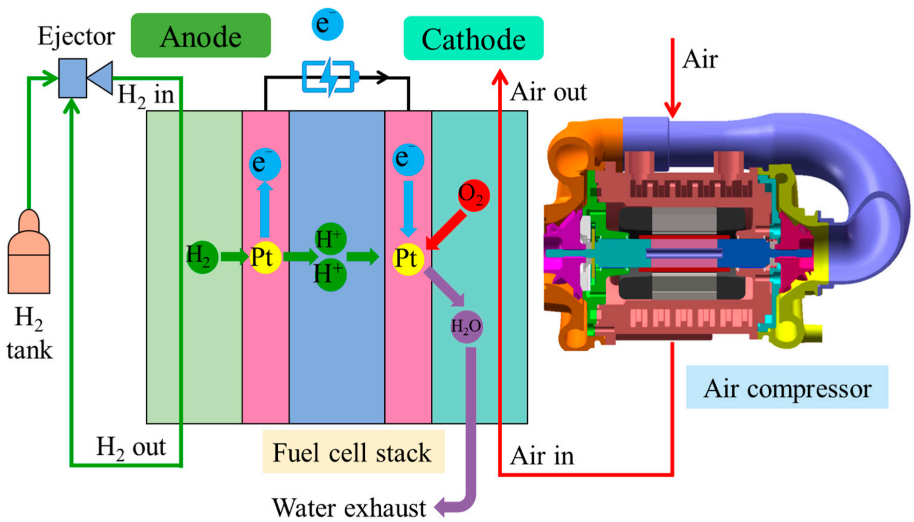

Figure 1. Air compressor in HFCVs.

Among these components, the air compressor is a crucial rotating component within the cathode power generation system of hydrogen vehicles. It ensures that the air supplied to the stack for pressurization is clean and oil-free while also maintaining specific pressure ratios and flow rates. The interaction between air compressors and the fuel cell stack is vital for the overall performance of the system. The air compressor must deliver oxygen to the fuel cell stack at appropriate pressure and temperature levels to guarantee the overall system performance [2,4]. Fuel cell systems often encounter varying power demands, and the air compressor must exhibit flexibility to ensure a continuous and suitable air supply to the fuel cell stack [6]. Effective integration with the control system is paramount, ensuring an air supply that meets the dynamic demands of the fuel cell stack [19]. In the air compressor, the permanent magnet synchronous motor directly drives the rotor system, allowing maximum speeds of up to 100,000 rpm. Two gas foil radial bearings utilize an effective dynamic pressure gas film to levitate the rotor system, ensuring stable operation that is oil-free at ultra-high speeds for the air supply system in HFCVs.

2.2. Content and Methodologies Employed in the Research

In this paper, multi-objective optimization of operational characteristics of the air compressor utilized in hydrogen-powered vehicles is conducted to guide its efficient and stable operation. There are five parts including design experiments, sensitivity analysis, performance analysis, multi-objective optimization, and optimization verification, as presented in Figure 2.

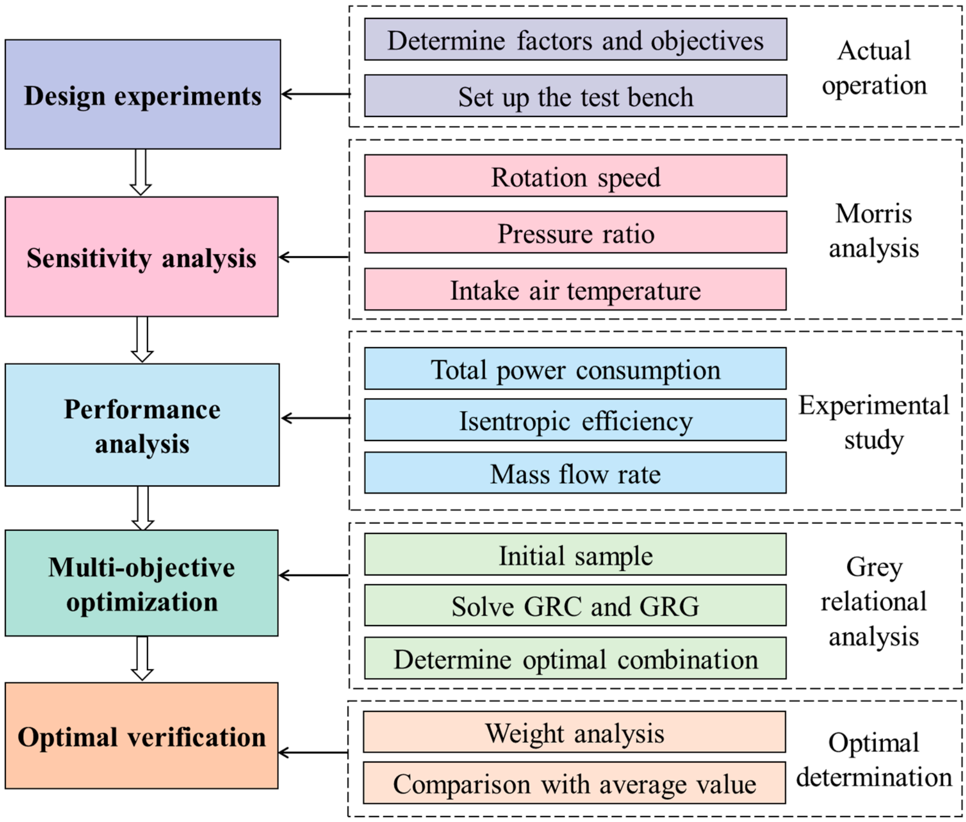

Figure 2. Methodology in this study.

Firstly, the experimental setup is built to assess the performance of the air compressor under real operating conditions in HFCVs. The second part focuses on examining the influence magnitude of operational parameters on the optimization objectives using the Morris sensitivity analysis. Thirdly, the research investigates the impact mechanisms of operational parameters on objective parameters based on the experimental results. Fourthly, employing grey relational analysis and targeting a higher efficiency, larger flow rate, and lower energy consumption as optimization objectives, the study obtains the optimal operational combination for the air compressor. Finally, through weight analysis and comparison with average values, the optimal operational condition of the air compressor applied in hydrogen energy vehicles is verified to improve efficiency and stability.

3. Experimental Bench and Theoretical Model

3.1. Experimental Bench

3.1.1. Experimental Setup

The experimental setup for the air compressor employing a two-stage centrifugal mechanism is depicted in Figure 3. Filtered air enters the first stage of the centrifugal compressor. It undergoes compression across two stages before the compressed gas is discharged into the atmosphere. The experiment utilizes a DC power cabinet to supply power to the air compressor. A controller interfaces with control software on a computer to manage the operational parameters of the compressor. The gas pressure at the inlet and outlet of the compressor is monitored and recorded using pressure gauges, and the temperature is measured using temperature sensors. The exhaust flow rate is measured using a vortex flowmeter. The arrangement of all instruments and pipelines follows the corresponding international standards, ensuring the reliability of the measurement results. More information about the equipment and appliances is summarized in Table 1.

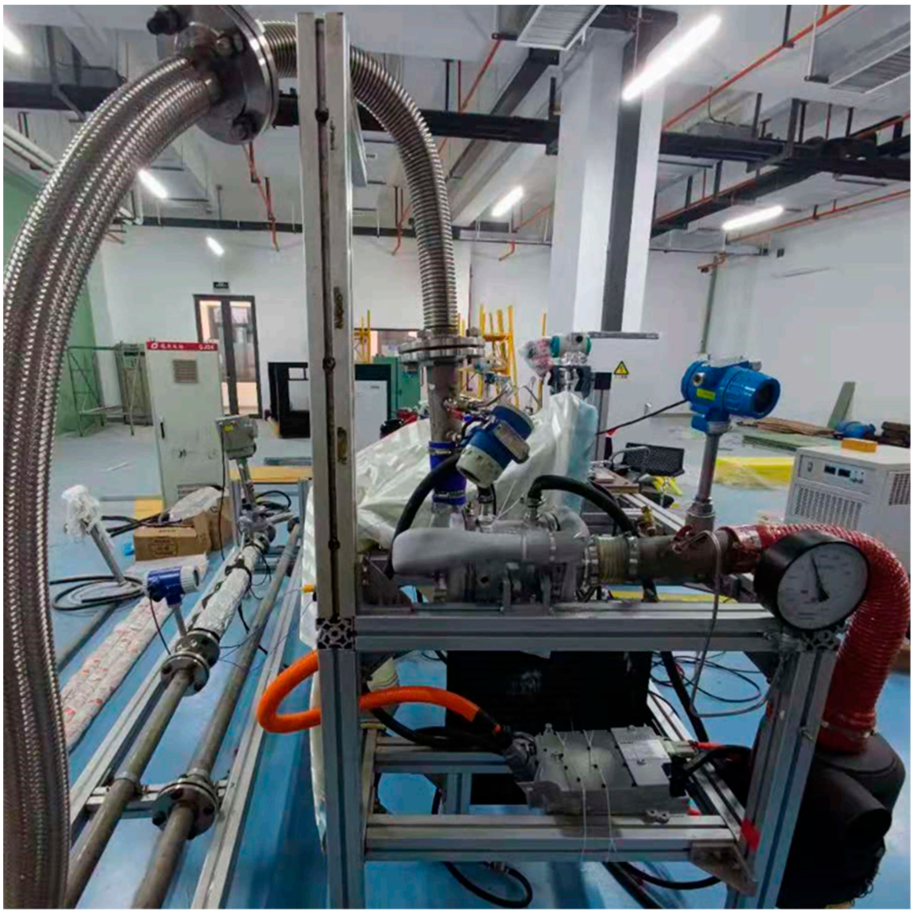

(**a**)

Figure 3. *Cont.*

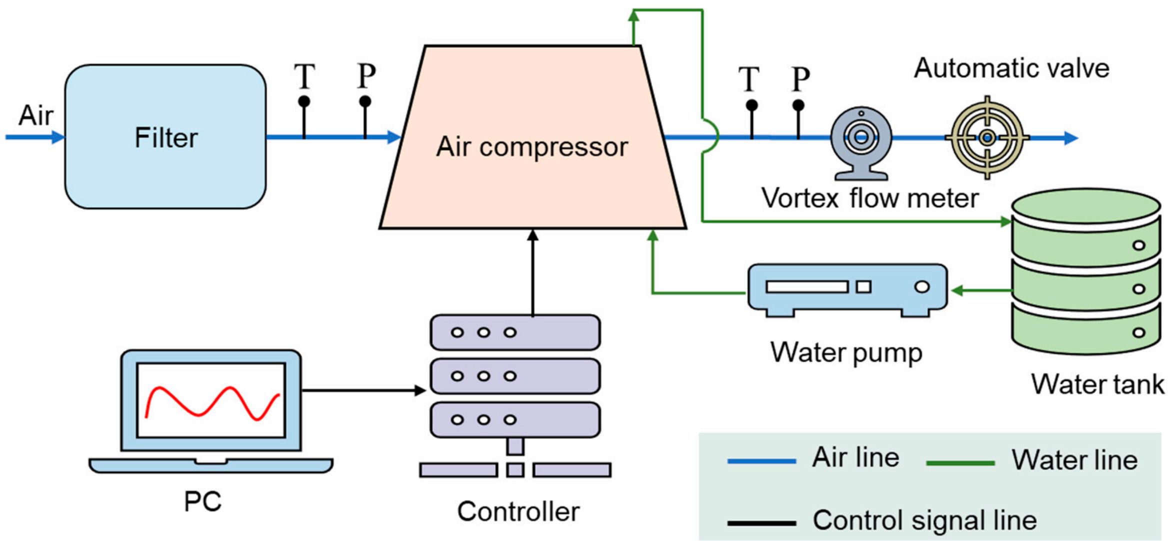

(**b**)

Figure 3. Experimental setup of air compressor: (**a**) actual bench and (**b**) schematic diagram.

Table 1. Detailed information on the equipment and appliances of the air compressor.

No.	Equipment and Appliances	Limit	Precision
1	Filter	≥0.003 µm	/
2	Centrifugal compressor	20,000–90,000 rpm, 0.01–0.162 kg/s	/
3	Compressor controller	180–445 VDC	±200 rpm
4	DC power cabinet	500 V	±1%
5	Automatic valve	0–1	/
6	Temperature transducer	300 °C	±1 °C
7	Pressure transducer	0.6 MPa	±0.2%
8	Vortex flow meter	30–500 m^3/h	±1%

3.1.2. Theoretical Calculation of Air Compressor

To address the issue of high energy consumption and poor stability in existing centrifugal air compressors for hydrogen vehicles, a study focused on developing an optimal air compressor with a lower energy consumption, higher isentropic efficiency, and a larger mass flow rate is conducted.

The isentropic compression work of the air compressor is calculated as Equation (1) based on isentropic compression work W_s, adiabatic index k, gas constant R, and intake temperature T_1 [31]:

$$W_s = \frac{k}{k-1} R T_1 \left[\left(\frac{p_2}{p_1} \right)^{\frac{k-1}{k}} - 1 \right] \tag{1}$$

The shaft power W_{tot} represents the total power consumption, which is expressed by Equation (2):

$$W_{tot} = P \times \eta_{mo} \tag{2}$$

where P is the power displayed on the DC power cabinet and η_{mo} is the motor efficiency.

Isentropic efficiency η can be expressed as Equation (3) [14]:

$$\eta = \frac{W_s}{W_{tot}} \tag{3}$$

3.2. Theoretical Model

3.2.1. Global Sensitivity Analysis

The Morris sensitivity analysis technique is commonly employed to evaluate the sensitivity of input factors globally. It determines the influence grade of input factors on the output results by calculating sensitivity coefficients for each factor. It is considered a highly effective method for identifying sensitive and insensitive parameters. In this study, the impact of operating parameters on the optimization objectives based on the Morris method is obtained to guide the efficient control of the air supply system used in HFCVs.

In the Morris sensitivity analysis, the utilization of elementary effects can be used to quantify the influence grade of a single perturbation on the objectives. Equation (4) allows for the calculation of the elementary effect of the i_{th} input parameter [26]:

$$S_i = \frac{y(x_1, x_2, \ldots, x_i + \Delta x, \ldots, x_n) - y(x_1, x_2, \ldots, x_n)}{\Delta x} \tag{4}$$

The average value μ_i determines the assessment of the input parameter influence on the optimization objectives. A higher μ_i signifies a greater impact of the input parameters on the objective. Therefore, the average value can be expressed as [24]:

$$\mu_i = \frac{1}{m} \sum_{j=1}^{m} S_{ij} \tag{5}$$

Taking into account the impact of negative values on the average, a corrected average is used to represent sensitivity. Therefore, the corrected average can be expressed as [24]:

$$\mu_i{}^* = \frac{1}{m} \sum_{j=1}^{m} |S_{ij}| \tag{6}$$

where S_i is the elementary effect of the i_{th} input factor, $y(x_1, x_2, \ldots, x_n)$ is the initial output result, $y(x_1, x_2, x_i + \Delta x \ldots, x_n)$ is the output result after the perturbation of the input factor, Δx is the perturbation of the input factor, and m represents the quantity of autonomous random pathways utilized in the global sensitivity analysis.

3.2.2. Initial Sample and Multi-Objective Optimization

Determining the initial sample set is the first step in conducting multi-objective optimization [32]. An orthogonal array is a design method used to study the impact of multiple factors on objectives within the fewest possible experiments, effectively analyzing the relationships between factors and objectives and ensuring the validity of the analysis results. Due to the presence of three input factors in this study, an orthogonal design table L_9 (3^4) is employed as the initial sample set [33,34]. It should be emphasized that experts design orthogonal arrays, and researchers need to choose a reasonable orthogonal table according to the specific research content to obtain comprehensive and reasonable results [34].

The key to grey relational analysis (GRA) is to calculate the grey relational grade (GRG) of integrated parameters based on weighted allocation in multi-objective scenarios [35]. A higher grey relational grade indicates better outcomes [27].

Firstly, the multi-objective parameters $y_i(k)$ obtained from the orthogonal array undergo normalization. Equations (7) and (8) are used for objectives favoring larger and smaller values, respectively:

$$X_i(k) = \frac{y_i(k) - \min(y_i(k))}{\max(y_i(k)) - \min(y_i(k))} \tag{7}$$

$$X_i(k) = \frac{max(y_i(k)) - y_i(k)}{\max(y_i(k)) - \min(y_i(k))} \tag{8}$$

The grey relational coefficient γ can be expressed as [26]:

$$\gamma(\mathrm{X}_{0i}, X_i(\mathrm{k})) = \frac{\Delta_{min} + \zeta\Delta_{max}}{\Delta_{ik} + \zeta\Delta_{max}} \tag{9}$$

$$\Delta_{ik} = |X_{0i} - X_i(k)| \tag{10}$$

$$\Delta_{min} = min\{\Delta_{ik}\} \tag{11}$$

$$\Delta_{min} = max\{\Delta_{ik}\} \tag{12}$$

where ζ is the weight coefficient assigned to objectives, ranging from 0 to 1.

A larger grey relational degree $\delta(R_0, R_k)$ indicates better results, and it is calculated as [26,27]:

$$\beta_i = \frac{1 - T_i}{\sum_i^{N_{qc}}(1 - T_i)} i = 1, 2, \ldots, N_{qc} \tag{13}$$

$$T_i = -\frac{\sum_{k=1}^{N_{ex}} p_{ik} ln p_{ik}}{ln N_{ex}} \tag{14}$$

$$p_{ik} = \frac{\gamma(\mathrm{X}_{0i}, X_i(\mathrm{k}))}{\sum_{k=1}^{N_{ex}} \gamma(\mathrm{X}_{0i}, X_i(\mathrm{k}))} k = 1, 2, \ldots, N_{ex} \tag{15}$$

$$\delta(\mathrm{R}_0, \mathrm{R}_k) = \sum_{i=1}^{N_{qc}} \beta_i \gamma(\mathrm{X}_{0i}, X_i(\mathrm{k})) \tag{16}$$

where N_{ex} is the number of the experiment, and N_{qc} is the number of the objective.

4. Results and Discussions

In this study, the operational parameters, including rotation speed, pressure ratio, and intake air temperature, are selected based on previous investigations [17]. It should be noted that the total power consumption, corrected mass flow rate, and isentropic efficiency are considered the optimization objectives for the air compressor to optimize the dynamic performance of the hydrogen energy vehicles [11].

4.1. Sensitivity Analysis

The impact of operational parameters on the total power consumption of the air compressor in hydrogen energy vehicles is illustrated in Figure 4. Based on the results, the rotational speed exhibits the highest sensitivity to total power consumption. In contrast, the pressure ratio and intake air temperature demonstrate a comparable level of sensitivity to total power consumption. It is noteworthy that the impact of rotational speed on total power consumption significantly surpasses that of the pressure ratio and intake air temperature. This is because the total power consumption is primarily determined by the permanent magnet synchronous motor, and the rotational speed represents the most influential factor affecting the energy consumption of the motor. Therefore, to reduce the power usage of the air compressor and enhance the energy efficiency of HFCVs, efforts should be made to operate the air compressor at lower rotational speeds whenever possible.

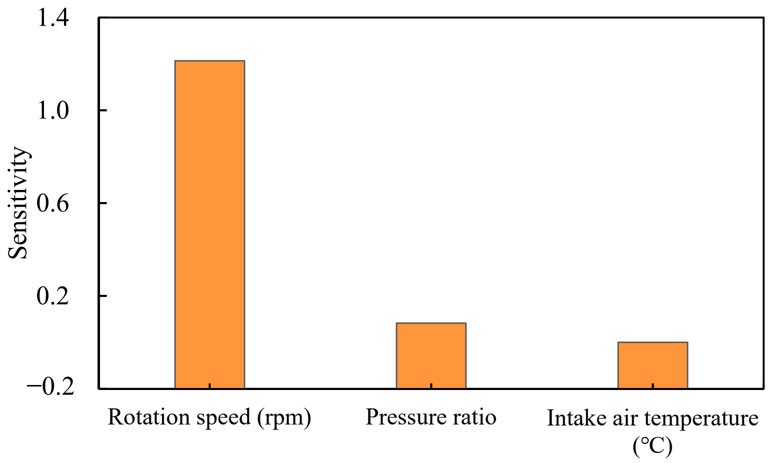

Figure 4. The sensitivity of operational parameters to total power consumption.

The sensitivity analysis results of operational parameters on the efficiency under isentropic conditions in a dual-stage centrifugal air compressor are depicted in Figure 5. Among these factors, the pressure ratio exhibits the most pronounced sensitivity to the isentropic efficiency, followed by rotational speed, while the intake air temperature has the least impact. This is because the pressure ratio directly influences the adiabatic compression work of the centrifugal air compressor. Moreover, the pressure ratio should be prioritized for adjustment as the primary factor when targeting high isentropic efficiency. In comparison to the influence of the pressure ratio and rotational speed on isentropic efficiency, the impact of the inlet temperature is minimal.

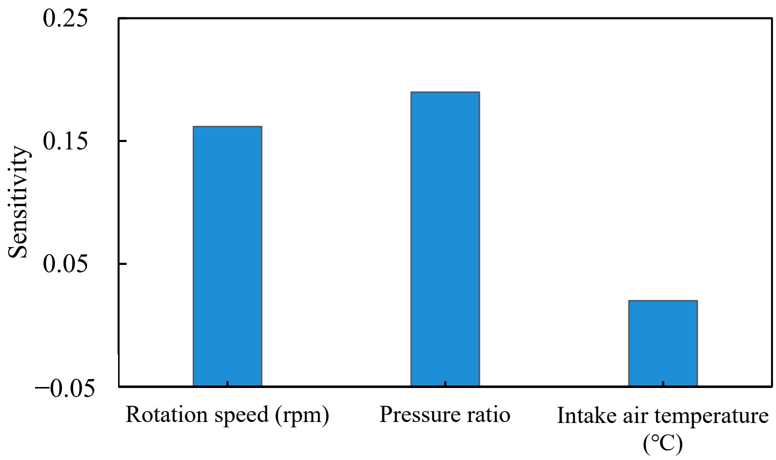

Figure 5. The sensitivity of operational parameters to isentropic efficiency.

The sensitivity analysis of operational parameters on the corrected mass flow rate of the air compressor in hydrogen energy vehicles is illustrated in Figure 6. The research findings indicate that the pressure ratio has the most significant impact on the mass flow rate of the air compressor, followed closely by the rotational speed, and the influence of inlet temperature on the flow rate is minimal. Therefore, the primary adjustment should focus on modifying the pressure ratio of the compressor when hydrogen-powered vehicles require higher mass flow rates from the air compressor to the stack. Furthermore, simultaneous adjustments, including the pressure ratio and the rotational speed of the air compressor, could be considered to meet the larger flow rate requirements of the fuel cell stack.

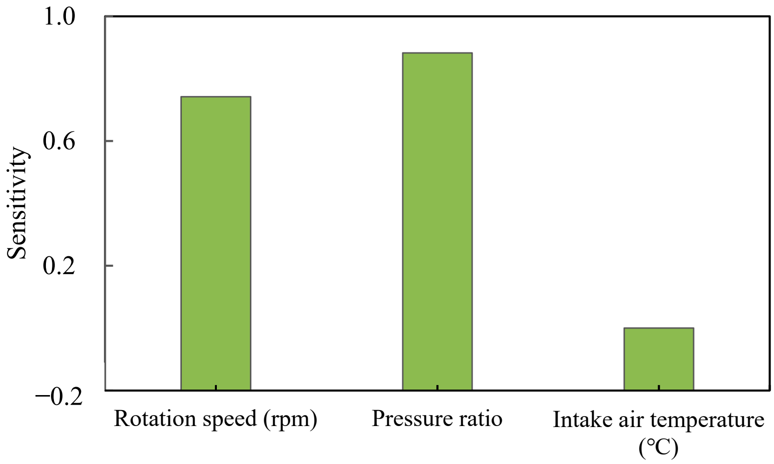

Figure 6. The sensitivity of operational parameters to corrected mass flow.

Based on the above results and discussions, it is evident that the Morris global sensitivity analysis accurately identifies the impact magnitude of operational parameters on the objective variables. When hydrogen energy vehicles exhibit varying demands on the air compressor, the Morris sensitivity analysis results effectively guide the efficient operation of the air compressor to meet the specific requirements of the fuel cell stack. However, further discussion and research are required to investigate the effects of operational parameters on the optimization objectives of the air compressor.

4.2. Impact of Operational Parameters on the Performance of the Air Compressor

4.2.1. Total Power Consumption

The influence of operational parameters on the total power consumption of the two-stage centrifugal air compressor is depicted in Figure 7. The research findings indicate that the total power consumption increases with a higher rotational speed and intake air temperature. It is noteworthy that with an increase in the pressure ratio, the total power consumption initially rises before subsequently decreasing. It is noteworthy that the total power consumption increases first and then decreases with the increase in the pressure ratio. This means that a specific pressure ratio exists at which the total power consumption of the air compressor reaches its maximum, which is undesirable for achieving low-energy operation of the compressor and should be avoided as much as possible. In this experiment, the pressure ratio corresponding to the maximum energy consumption is 2.3. Considering the sensitivity analysis of operational parameters on total power consumption, the primary step would be to decrease the rotational speed to reduce the energy utilized by the air compressor.

4.2.2. Isentropic Efficiency

The impact of operational parameters on the isentropic efficiency of the air compressor is illustrated in Figure 8. An analysis reveals that the isentropic efficiency increases with higher values of the rotational speed, pressure ratio, and inlet temperature. In this experiment, the maximum isentropic efficiency is observed at a rotational speed of 90,000 rpm, a pressure ratio of 2.9, and an intake air temperature of 20.7 °C. Taking into account both the sensitivity analysis of operational parameters on isentropic efficiency and their specific impact, the primary step should be to increase the rotational speed when high isentropic efficiency is required from the air compressor.

4.2.3. Corrected Mass flow Rate

The specific trend of operational parameters on the corrected mass flow rate of the air compressor is depicted in Figure 9. This study reveals that the mass flow rate increases as the rotational speed increases. However, as the pressure ratio and inlet temperature increase, the mass flow rate decreases. Combining the sensitivity analysis of operational parameters on the air compressor's mass flow rate and their specific impact trends, the initial step would involve decreasing the pressure ratio and increasing the rotational speed when the fuel cell stack requires high flow rates from the air compressor. On the contrary, it is recommended to decrease the rotational speed to achieve a higher pressure ratio.

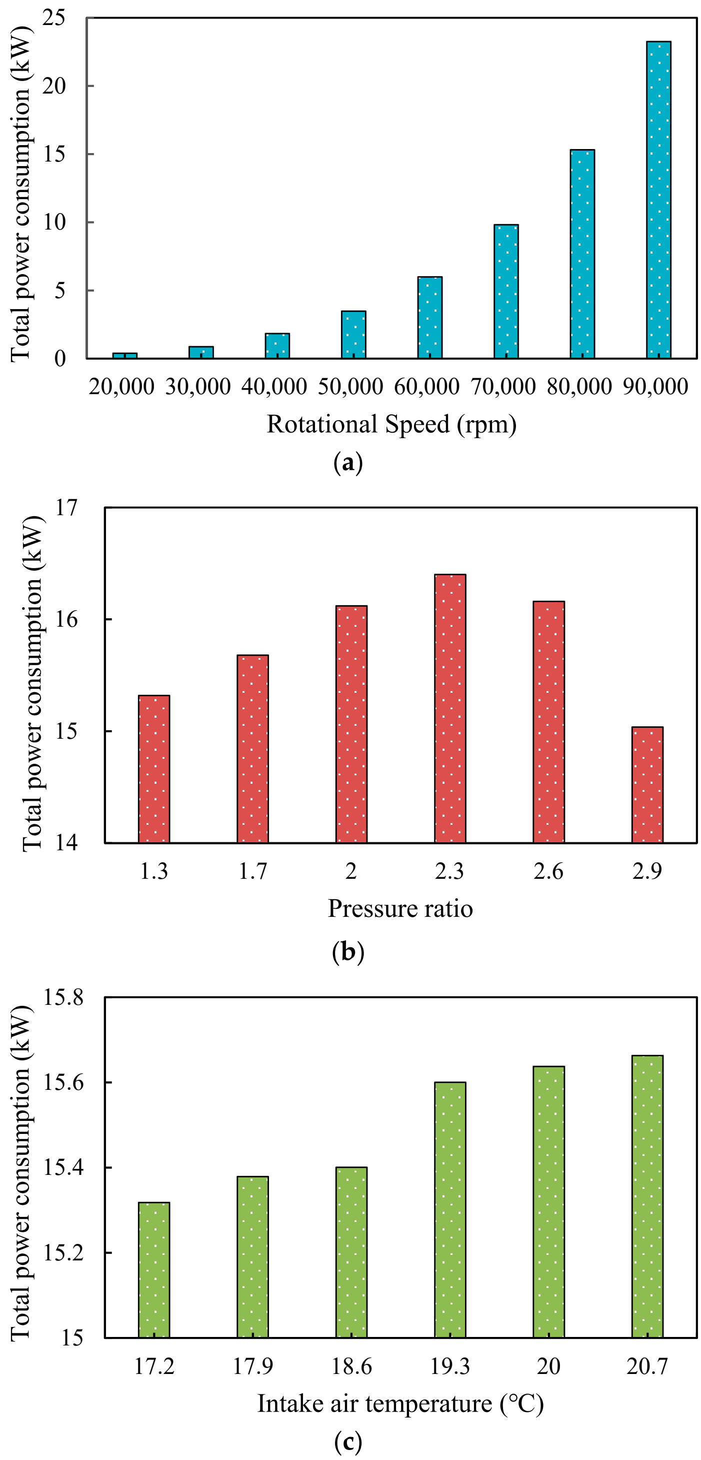

Figure 7. The effects of operating parameters on total power consumption: (**a**) rotational speed, (**b**) pressure ratio, and (**c**) intake air temperature.

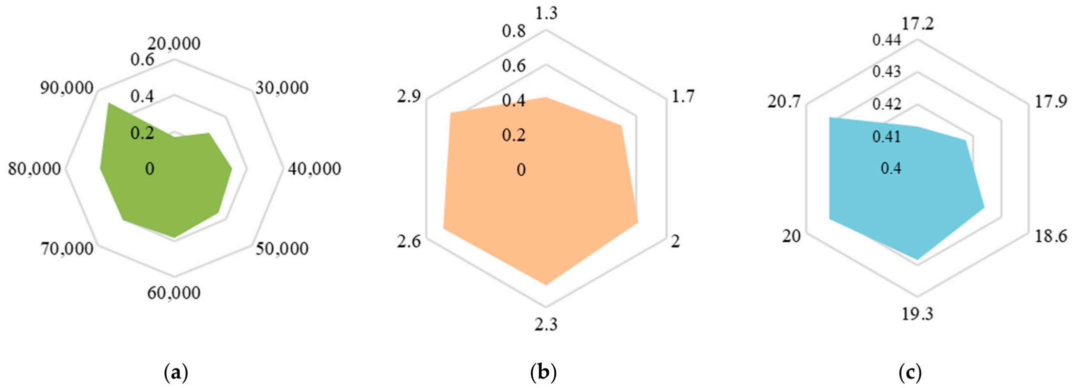

Figure 8. The effects of operating parameters on isentropic efficiency: (**a**) rotational speed, (**b**) pressure ratio, and (**c**) intake air temperature.

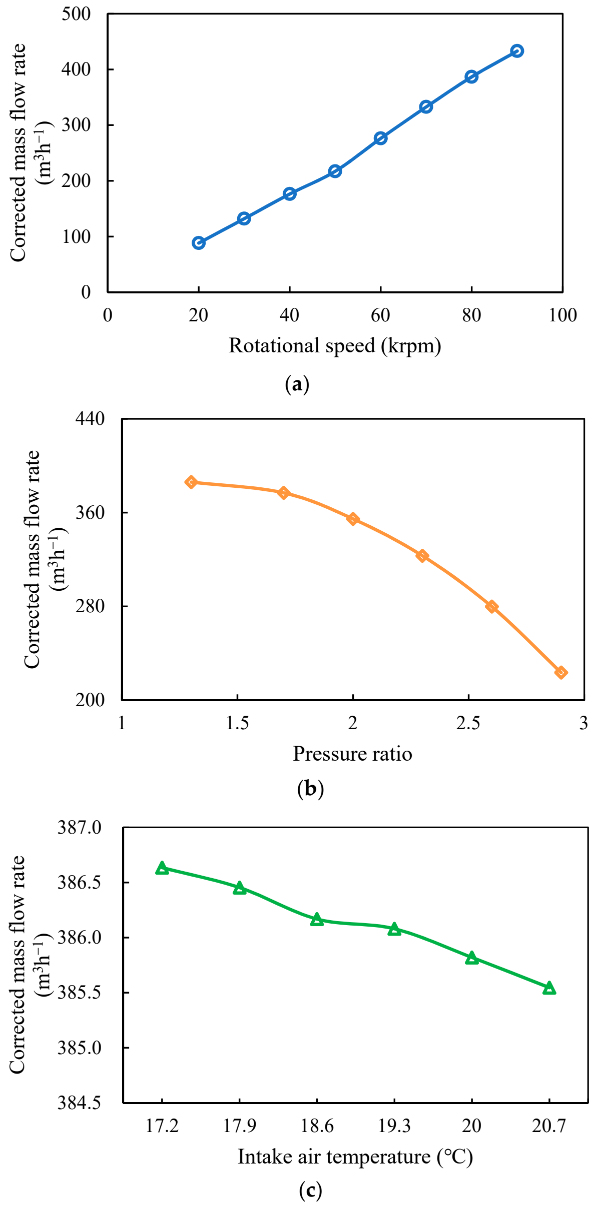

Figure 9. The effects of operating parameters on corrected mass flow rate: (**a**) rotational speed, (**b**) pressure ratio, and (**c**) intake air temperature.

4.3. Results of Multi-Objective Optimization

4.3.1. Initial Sample

To achieve a high-efficiency and energy-saving operation in HFCVs, the air compressor within the cathode air system is required to possess the characteristics of having a higher flow rate, larger efficiency, and lower power consumption. Based on prior research [17,19,21], the rotational speed, pressure ratio, and intake air temperature are chosen as factors, while high efficiency, low energy consumption, and high mass flow rate are selected as optimization objectives. The levels of each factor are shown in Table 2. Based on the orthogonal design table L_9 (3^4) and Table 2, the initial sample set is illustrated in Table 3 [34]. The objective parameters under the initial samples are depicted in Figure 10.

Table 2. Levels of each factor.

Factors	Levels		
	1	2	3
Rotational speed/rpm	20,000	50,000	80,000
Intake air temperature/°C	18.3	18.8	19.3
Pressure ratio	1.0	1.4	1.8

Table 3. Initial sample based on orthogonal array L_9 (3^4).

No.	Operational Parameters		
	Rotational Speed/rpm	Intake Air Temperature/°C	Pressure Ratio
1	20,000	18.3	1.0
2	20,000	18.8	1.4
3	20,000	19.3	1.8
4	50,000	18.3	1.4
5	50,000	18.8	1.8
6	50,000	19.3	1.0
7	80,000	18.3	1.8
8	80,000	18.8	1.0
9	80,000	19.3	1.4

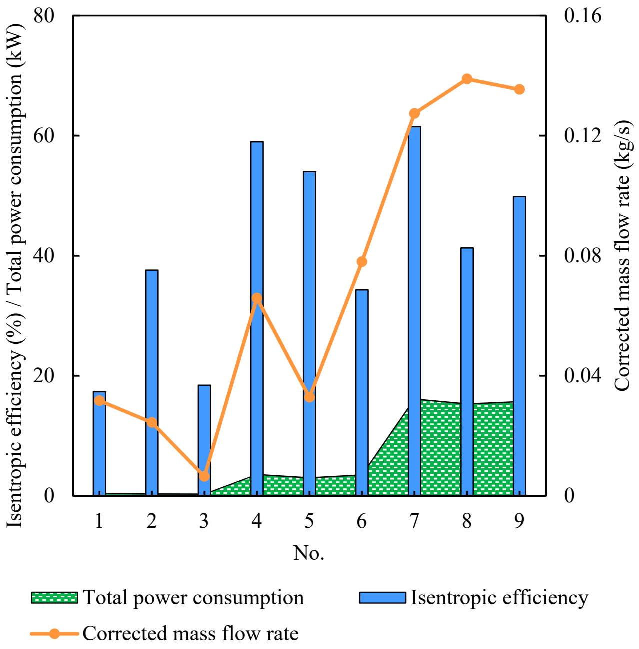

Figure 10. Objective parameters under the initial sample.

4.3.2. Multi-Objective Optimization Results

The multi-objective optimization results considering both high isentropic efficiency and low power dissipation (Optimization A) are illustrated in Figure 11 based on the GRA theory formulas. The maximum GRG of 0.7937 is achieved for the initial sample No. 4. At this point, the isentropic efficiency is 58.97%, the total power consumption is 3.56 kW, and the mass flow rate is 0.066 kg/s.

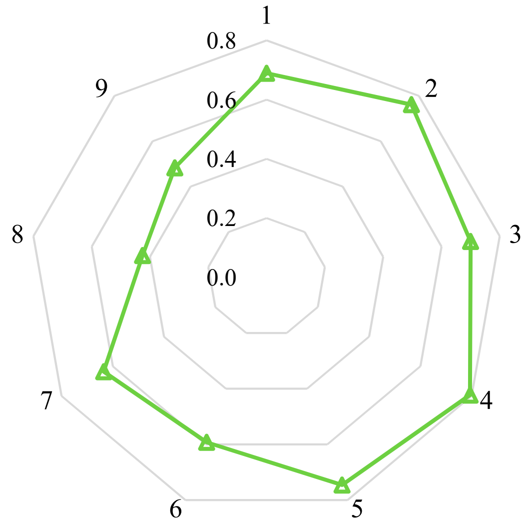

Figure 11. Multi-objective optimization results in high efficiency and low energy consumption.

When considering both high mass flow rate and low energy consumption simultaneously (Optimization B), the solution for the GRG in the multi-objective optimization is shown in Figure 12. The maximum GRG of 0.6873 is discovered for the initial sample No. 8. At the maximum GRG, the mass flow rate is 0.1389 kg/s, the total power consumption is 15.32 kW, and the isentropic efficiency is 41.30%.

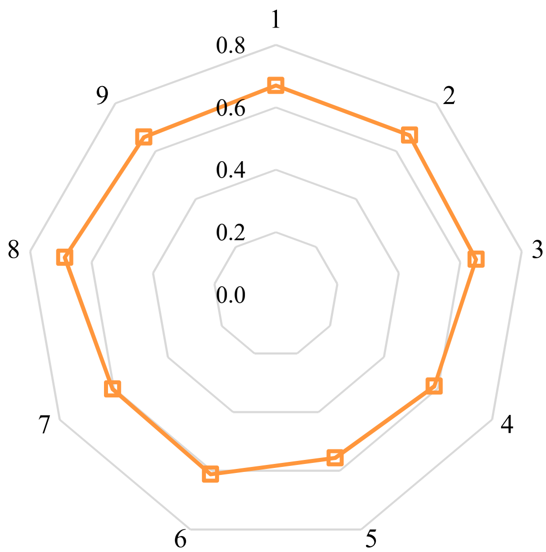

Figure 12. Multi-objective optimization results in high mass flow rate and low energy consumption.

However, the optimized results considering high flow rate, high efficiency, and low energy consumption simultaneously (Optimization C) are illustrated in Figure 13. The results indicate that the maximum GRG of 0.734 is achieved for the initial sample No. 7.

At the optimal operating parameters, the isentropic efficiency is 61.48%, the total power consumption is 16.12 kW, and the mass flow rate is 0.1274 kg/s.

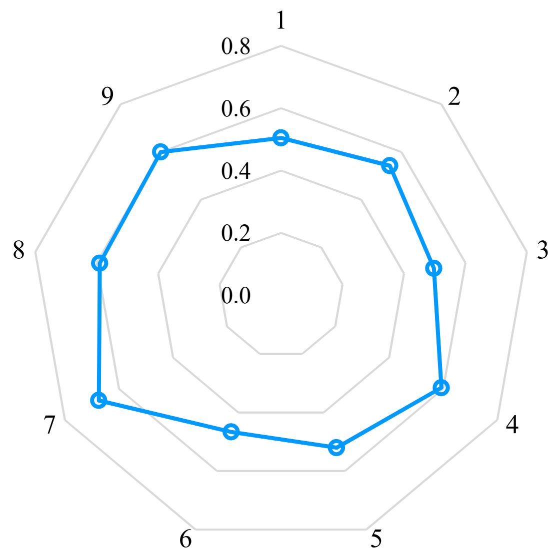

Figure 13. Multi-objective optimization results in high efficiency, large flow rate, and low energy consumption.

4.4. Optimal Combination Verification

Table 4 illustrates the optimal operational parameters of the air compressor under different optimization objectives. The results indicate substantial differences in the optimal operational parameters when varying weights are assigned to total power consumption, isentropic efficiency, and mass flow rate as optimization objectives. In engineering applications, researchers can utilize the grey relational optimization theory to adjust the weights assigned to different objectives, thereby making corresponding adjustments to the operational parameters of the air compressor. This approach aims to achieve high efficiency and energy conservation in the operation of the air compressor.

Table 4. Optimum operational combinations of the air compressor under different objectives.

Weight	Optimization A	Optimization B	Optimization C
Total power consumption ↓	0.45	0.48	0.35
Isentropic efficiency ↑	0.55	0	0.35
Corrected mass flow rate ↑	0	0.52	0.30
Optimal combination	No. 4	No. 8	No. 7

Note: ↓ the smaller, the better. ↑ the larger, the better.

As shown in Figure 14, compared to the initial sample average values (isentropic efficiency 41.48%, total power consumption 6.463 kW, 0.0712 kg/s), Optimization A demonstrates a notable 42.18% enhancement in isentropic efficiency and a substantial 44.92% reduction in energy consumption. Optimization B results in a significant 95.1% increase in mass flow rate. Optimization C achieves a remarkable 78.88% elevation in mass flow rate and a 48.23% improvement in isentropic efficiency while only experiencing a 50% rise in energy consumption. The validation results indicate that Optimization A significantly reduces energy consumption aimed at lowering the power consumption of the air compressor, thereby enhancing its energy efficiency. The significant increase in mass flow rate and isentropic efficiency achieved by Optimization B and Optimization C substantiates the air compressor's optimization outcomes under varying requirements. This analysis and discussion thoroughly validate the optimization results for different demands on the air compressor.

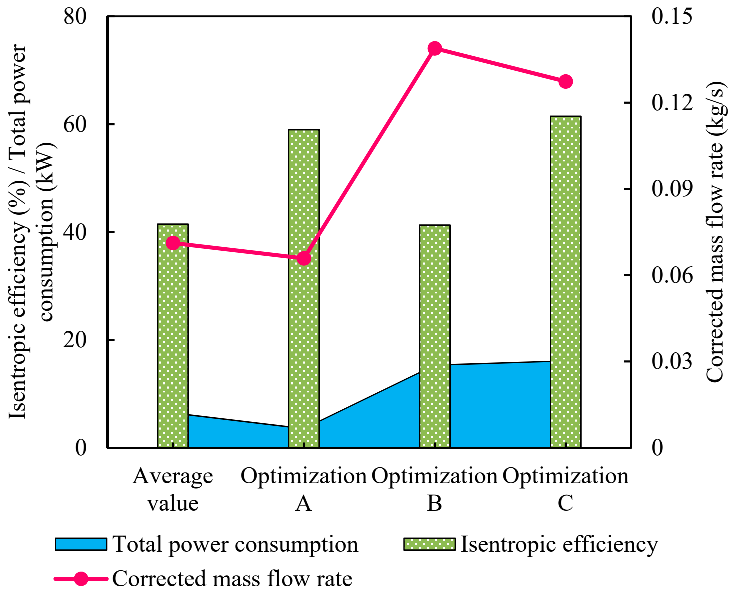

Figure 14. Comparison of the optimization results with the initial sample average values.

4.5. Constraints and Future Investigations

This study provides novel insights and discoveries for the efficient and reliable operation of air compressors in HFCVs. However, there are still limitations in the research that require further in-depth investigation in the future. Therefore, the directions for future research are: (1) the effects of unexpected operating conditions and component failures on the experimental results need to be considered, especially in optimal operational parameters. (2) Integrating fault tolerance and robustness theories to conduct a robustness analysis and the testing of optimal results.

5. Conclusions

This paper investigated the global sensitivity and multi-objective optimization of the operational parameters of the air compressor in hydrogen energy vehicles based on experimental results. These findings hold significant value in guiding the efficient and stable operation of air compressors. The main conclusions are summarized as follows.

1. The rotational speed exhibits the highest sensitivity to total energy consumption, while the pressure ratio showcases the most prominent sensitivity towards the isentropic efficiency and mass flow rate. Conversely, the impact of the intake temperature on energy consumption, efficiency, and flow rate is minimal.
2. The total power consumption increases with higher rotational speed and inlet temperature. Notably, with an increase in the pressure ratio, total power consumption initially rises before decreasing. Isentropic efficiency increases with higher values of rotational speed, pressure ratio, and intake temperature. As rotational speed increases, mass flow rate increases. However, with an increase in the pressure ratio and intake temperature, the mass flow rate decreases.
3. Considering high efficiency and low energy consumption, the optimal combination of operational parameters is a rotational speed of 50,000 rpm, a pressure ratio of 1.4, and an intake temperature of 18.3 °C. At these optimal operational parameters, the isentropic efficiency improved by 42.18%, while power consumption decreased by 44.92%.
4. Considering the high mass flow rate and low energy consumption, the optimal combination of operational parameters is a rotational speed of 80,000 rpm, a pressure ratio of 1.0, and an intake temperature of 18.8 °C. At these optimal operational parameters, the mass flow rate increased by 95.1%.

5. When considering a high flow rate, high efficiency, and low energy consumption simultaneously, the optimal combination of operational parameters is a rotational speed of 80,000 rpm, a pressure ratio of 1.8, and an intake temperature of 18.3 °C. Compared to the average values, at half the increase in power consumption, the mass flow rate increased by 78.88%, and the isentropic efficiency increased by 48.23%.

The research findings mentioned above provide valuable insights into the efficient operation of the air compressor under various demands from the fuel cell stack. The comprehensive multi-factor, multi-objective research method proposed in this paper is applicable to other optimization studies concerning air compressors in HFCVs. In addition, air compressors can be affected by transient conditions, including start–stop phases, load fluctuations, sudden pressure changes, and temperature variations. To address these, advanced control systems, variable speed drives, system modeling, optimized component design, and monitoring with predictive maintenance need to be investigated further to enhance efficiency and stability.

Author Contributions: T.S.: conceptualization, data curation, formal analysis, writing—original draft, writing—review and editing; X.P.: project administration, writing—review and editing. All authors have read and agreed to the published version of the manuscript.

Funding: This paper is supported by the National Natural Science Foundation of China (Grant No. 52276036).

Institutional Review Board Statement: Not applicable.

Informed Consent Statement: Not applicable.

Data Availability Statement: The data presented in this study are available on request from the corresponding author. The data are not publicly available due to privacy.

Conflicts of Interest: The authors declare that they have no known competing financial interests or personal relationships that could have appeared to influence the work reported in this paper.

References

1. Van Rensburg, T.M.; Brennan, N.; Howard, A. Tourist preferences for fuel cell vehicle rental: Going green with hydrogen on the island of tenerife. *Int. J. Hydrogen Energy* **2023**, *48*, 29350–29366. [CrossRef]
2. Nanmaran, R.; Mageswari, M.; Srimathi, S.; Ganesh Raja, G.; Al Obaid, S.; Ali Alharbi, S.; Elumalai, P.; Thanigaivel, S. Mathematical modelling of hydrogen transportation from reservoir tank to hydrogen fuel cell electric vehicle (fcev) tank. *Fuel* **2024**, *361*, 130725. [CrossRef]
3. Park, S.; Lee, S. Theoretical analysis for improving the efficiency of ht-pemfc through unreacted hydrogen circulation. *Appl. Sci.* **2023**, *13*, 9292. [CrossRef]
4. Yang, R.; Zhang, W.; Li, S.; Xu, M.; Huang, W.; Qin, Z. Finite element analysis and optimization of hydrogen fuel cell city bus body frame structure. *Appl. Sci.* **2023**, *13*, 10964. [CrossRef]
5. Mori, M.; Iribarren, D.; Cren, J.; Cor, E.; Lotrič, A.; Gramc, J.; Drobnič, B.; Rey, L.; Campos-Carriedo, F.; Puig-Samper, G.; et al. Life cycle sustainability assessment of a proton exchange membrane fuel cell technology for ecodesign purposes. *Int. J. Hydrogen Energy* **2023**, *48*, 39673–39689. [CrossRef]
6. Akimoto, Y.; Shibata, M.; Tsuzuki, Y.; Okajima, K.; Suzuki, S. In-situ onboard evaluation and control of proton exchange membrane fuel cells using magnetic sensors. *Appl. Energy* **2023**, *351*, 121873. [CrossRef]
7. Thounthong, P.; Mungporn, P.; Guilbert, D.; Takorabet, N.; Pierfederici, S.; Nahid-Mobarakeh, B.; Hu, Y.; Bizon, N.; Huangfu, Y.; Kumam, P. Design and control of multiphase interleaved boost converters-based on differential flatness theory for pem fuel cell multi-stack applications. *Int. J. Electr. Power* **2021**, *124*, 106346. [CrossRef]
8. Liu, Q.; Xu, H.; Lin, Z.; Zhu, Z.; Wang, H.; Yuan, Y. Experimental study of the thermal and power performances of a proton exchange membrane fuel cell stack affected by the coolant temperature. *Appl. Therm. Eng.* **2023**, *225*, 120211. [CrossRef]
9. Deng, B.; Zhang, X.; Yin, C.; Luo, Y.; Tang, H. Improving a fuel cell system's thermal management by optimizing thermal control with the particle swarm optimization algorithm and an artificial neural network. *Appl. Sci.* **2023**, *13*, 12895. [CrossRef]
10. Pourrahmani, H.; Van Herle, J. Evaluation criterion of proton exchange membrane (ecpem) fuel cells considering inserted porous media inside the gas flow channel. *Appl. Therm. Eng.* **2022**, *203*, 117952. [CrossRef]
11. Hu, D.; Liu, J.; Yi, F.; Yang, Q.; Zhou, J. Enhancing heat dissipation to improve efficiency of two-stage electric air compressor for fuel cell vehicle. *Energy Convers. Manag.* **2022**, *251*, 115007. [CrossRef]
12. Hu, C.; Geng, K.; Yang, C.; Zhou, M.; Chen, H. Thermodynamics investigation and spike-stall identification based on energy loss of centrifugal compressor. *Int. J. Heat Mass. Tran.* **2021**, *166*, 120693. [CrossRef]

13. Ahsan, N.; Al Rashid, A.; Zaidi, A.A.; Imran, R.; Abdul Qadir, S. Performance analysis of hydrogen fuel cell with two-stage turbo compressor for automotive applications. *Energy Rep.* **2021**, *7*, 2635–2646. [CrossRef]
14. Li, Z.; Han, G.; Lu, X.; Huang, E.; Zhao, S. Improving the operating range using a centrifugal compressor with a tandem impeller. *Aerosp. Sci. Technol.* **2020**, *96*, 105548. [CrossRef]
15. Sun, J.; Zuo, Z.; Liang, Q.; Zhou, X.; Guo, W.; Chen, H. Theoretical and experimental study on effects of humidity on centrifugal compressor performance. *Appl. Therm. Eng.* **2020**, *174*, 115300. [CrossRef]
16. Zhao, D.; Xu, L.; Huangfu, Y.; Dou, M.; Liu, J. Semi-physical modeling and control of a centrifugal compressor for the air feeding of a pem fuel cell. *Energy Convers. Manag.* **2017**, *154*, 380–386. [CrossRef]
17. Wan, Y.; Guan, J.; Xu, S. Improved empirical parameters design method for centrifugal compressor in pem fuel cell vehicle application. *Int. J. Hydrogen Energy* **2017**, *42*, 5590–5605. [CrossRef]
18. Mirzaee, S.; Zheng, X.; Lin, Y. Improvement in the stability of a turbocharger centrifugal compressor by tip leakage control. Proceedings of the Institution of Mechanical Engineers. *Part D J. Automob. Eng.* **2017**, *231*, 700–714. [CrossRef]
19. Liu, Z.; Li, L.; Ding, Y.; Deng, H.; Chen, W. Modeling and control of an air supply system for a heavy duty pemfc engine. *Int. J. Hydrogen Energy* **2016**, *41*, 16230–16239. [CrossRef]
20. Fang, X.; Chen, W.; Zhou, Z.; Xu, Y. Empirical models for efficiency and mass flow rate of centrifugal compressors. *Int. J. Refrig.* **2014**, *41*, 190–199. [CrossRef]
21. Zhao, D.; Zheng, Q.; Gao, F.; Bouquain, D.; Dou, M.; Miraoui, A. Disturbance decoupling control of an ultra-high speed centrifugal compressor for the air management of fuel cell systems. *Int. J. Hydrogen Energy* **2014**, *39*, 1788–1798. [CrossRef]
22. Cho, J.; Song, S. Prediction of hydrogen-added combustion process in t-gdi engine using artificial neural network. *Appl. Therm. Eng.* **2020**, *181*, 115974. [CrossRef]
23. Campolongo, F.; Saltelli, A. Sensitivity analysis of an environmental model: An application of different analysis methods. *Reliab. Eng. Syst. Safe* **1997**, *57*, 49–69. [CrossRef]
24. Petersen, S.; Kristensen, M.H.; Knudsen, M.D. Prerequisites for reliable sensitivity analysis of a high fidelity building energy model. *Energy Build.* **2019**, *183*, 1–16. [CrossRef]
25. Liu, L.; Ao, T.; Zhou, L.; Takeuchi, K.; Gusyev, M.; Zhang, X.; Wang, W.; Ren, Y. Comprehensive evaluation of parameter importance and optimization based on the integrated sensitivity analysis system: A case study of the btop model in the upper min river basin, china. *J. Hydrol.* **2022**, *610*, 127819. [CrossRef]
26. Xiong, F.; Wei, B.; Xu, F. Identification of arch dam mechanical parameters based on sensitivity analysis and hooke–jeeves algorithm optimization. *Structures* **2022**, *46*, 88–98. [CrossRef]
27. Shi, T.; Chen, Z.; Zhang, J.; Peng, X.; Feng, J. Performances investigation and multi-objective optimization of gas foil bearings in hydrogen fuel cell vehicles. *Int. J. Energy Res.* **2022**, *46*, 18849–18865. [CrossRef]
28. Wang, P.; Meng, P.; Zhai, J.; Zhu, Z. A hybrid method using experiment design and grey relational analysis for multiple criteria decision making problems. *Knowl.-Based Syst.* **2013**, *53*, 100–107. [CrossRef]
29. Zheng, G.; Jing, Y.; Huang, H.; Gao, Y. Application of improved grey relational projection method to evaluate sustainable building envelope performance. *Appl. Energy* **2010**, *87*, 710–720. [CrossRef]
30. Kuo, Y.; Yang, T.; Huang, G. The use of grey relational analysis in solving multiple attribute decision-making problems. *Comput. Ind. Eng.* **2008**, *55*, 80–93. [CrossRef]
31. Schröter, J.; Graf, T.; Frank, D.; Bauer, C.; Kallo, J.; Willich, C. Influence of pressure losses on compressor performance in a pressurized fuel cell air supply system for airplane applications. *Int. J. Hydrogen Energy* **2021**, *46*, 21151–21159. [CrossRef]
32. Yang, H.; Xu, Z.; Shi, Y.; Tang, W.; Liu, C.; Yunusa-Kaltungo, A.; Cui, H. Multi-objective optimization designs of phase change material-enhanced building using the integration of the stacking model and nsga-iii algorithm. *J. Energy Storage* **2023**, *68*, 107807. [CrossRef]
33. Zhang, Q.; Feng, J.; Zhang, Q.; Peng, X. Performance prediction and evaluation of the scroll-type hydrogen pump for fcvs based on cfd–taguchi method. *Int. J. Hydrogen Energy* **2019**, *44*, 15333–15343. [CrossRef]
34. Sabarish, K.V.; Parvati, T.S. An experimental investigation on l9 orthogonal array with various concrete materials. *Mater. Today Proc.* **2021**, *37*, 3045–3050. [CrossRef]
35. Zhu, H.; Liao, Q.; Qu, B.; Hu, L.; Wang, H.; Gao, R.; Zhang, Y. Relationship between the main functional groups and complex permittivity in pre-oxidised lignite at terahertz frequencies based on grey correlation analysis. *Energy* **2023**, *278*, 127821. [CrossRef]